



Synthesis and characterization of MCM-41-Biurea-Pd as a heterogeneous nanocatalyst and using its catalytic efficacy in C–C, C–N and C–O coupling reactions

Hana Batmani¹ | Nader Noroozi Pesyan¹ | Forugh Havasi²

¹Department of Organic Chemistry, Faculty of Chemistry, Urmia University, 57159 Urmia, Iran

²Department of Chemistry, Faculty of Sciences, University of Kurdistan, PO Box 66315-416, Sanandaj, Iran

Correspondence

Nader Noroozi Pesyan, Department of Organic Chemistry, Faculty of Chemistry, Urmia University, 57159 Urmia, Iran.
Email: nnp403@gmail.com

MCM-41-Biurea-Pd is introduced as a new, heterogeneous and reusable catalyst for C–C and C–heteroatom bond formation between various aryl halides, phenols and amines, in the presence of Ph₃SnCl (Stille reaction) in PEG-400 as a green solvent at room temperature. The structure of the functionalized MCM-41 was analysed using various techniques.

KEYWORDS

MCM-41-Biurea-Pd, nanocatalyst, Stille reaction

1 | INTRODUCTION

Paying attention to high surface area and facile recovery, nanoparticles have recently emerged as catalyst supports.^[1] As an important class of nanoparticles, porous materials perform a superior role in material science which is mainly due to their varied utilizations in size- and shape-selective applications. According to the IUPAC nomenclature classification, porous substances are divided into three categories: materials with (1) micropores (<2 nm), (2) mesopores (2–50 nm) and (3) macropores (>50 nm).^[2]

MCM-41 has been much studied because of its applications in nanoscience, environmental purification, catalysis, adsorption and drug delivery. The main reasons for this popularity are regular geometries, homogeneity of pores, high surface area, excellent thermal stability, tunability and accessibility of pores.^[3–8] These properties have led to many applications of MCM-41 for immobilizing acids,^[9] metal oxides,^[10] heteropoly acids,^[11] complexes,^[12] etc. Finally, in order to achieve various redox catalysts, it is also possible to introduce transition metals (e.g. Cr,^[13] VO,^[14] Mn,^[15] Cu,^[16] Ni^[17] and Pd^[18]) into the MCM-41 structure.

In modern organic chemistry, palladium-catalysed C–C bond formation reactions have taken on an essential role since their first development in the early 1970s.^[19] C–C coupling reactions catalysed by transition metals are among the most important reactions in organic synthesis.^[20–25] Among these reactions, C–C, C–O and C–N bond formations in cross-coupling reactions with palladium catalysts (e.g. Heck and Suzuki reactions) have become very effective tools in the pharmaceutical, agrochemical and fine-chemical industries.^[26–29]

Generally, the activity of homogeneous catalysts, for instance PdCl₂ and Pd(OAc)₂, are adequately high. However, their applications are limited mainly due to difficulties in their recovery and separation from a reaction mixture and their serious environmental pollution. Nanoparticles as recyclable catalysts are at the frontier between homogeneous and heterogeneous catalysis.^[30] To tackle the drawbacks of homogeneous catalysts, the development of heterogeneous palladium catalysts has significant theoretical and practical importance, and therefore it is one of the central objectives of green chemistry. Consequently, many solid materials such as zeolite, carbon, polymer materials and various forms of silica like mesoporous molecular sieves and amorphous

silica have been widely used for the immobilization of palladium catalysts.^[31–33]

This paper reports the preparation and characterization of a Pd(II) complex supported on biurea-functionalized nanostructured MCM-41 (MCM-41-Biurea-Pd) which is applied as a new and efficient catalyst for carbon–carbon and carbon–heteroatom coupling reactions.

2 | RESULTS AND DISCUSSION

In continuation of our current achievement in the introduction of novel nanocatalysts,^[17] herein we report the synthesis of MCM-41-Biurea-Pd as a novel and efficient catalyst for the coupling reaction of aryl halides, phenols and amines with Ph_3SnCl in PEG-400 at room temperature to afford biphenyls, aryl ethers and amines in high yields. The novel MCM-41-Biurea-Pd nanocatalyst was easily prepared as shown in Scheme 1.

2.1 | Catalyst Characterization

The synthesized catalyst was characterized using various methods. The small-angle X-ray diffraction (XRD) patterns of MCM-41, MCM-41-CPTMS (where CPTMS represents 3-chloropropyltrimethoxysilane), MCM-41-CPTMS-Biurea and MCM-41-CPTMS-Biurea-Pd are presented in Figure 1. Three peaks assigned to (100), (110) and (200) reflections observed are due to the hexagonal pore arrangement. After the functionalization steps, a reduction in intensity was observed in the XRD peaks. A reason might be the difference in the scattering contrast of the walls and the pores. These results may be attributed to the lower local order and increase in the wall thickness of the support materials.

Figure 2 shows the Fourier transform infrared (FT-IR) spectra of the synthesized MCM-41, MCM-41-CPTMS, MCM-41-CPTMS-Biurea and MCM-41-CPTMS-Biurea-

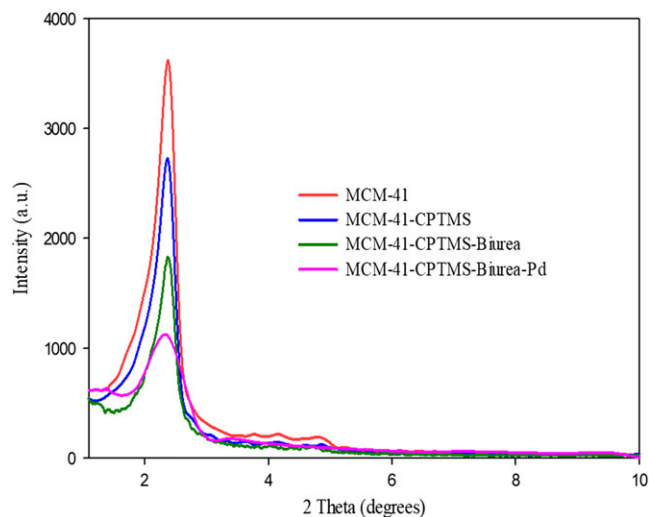
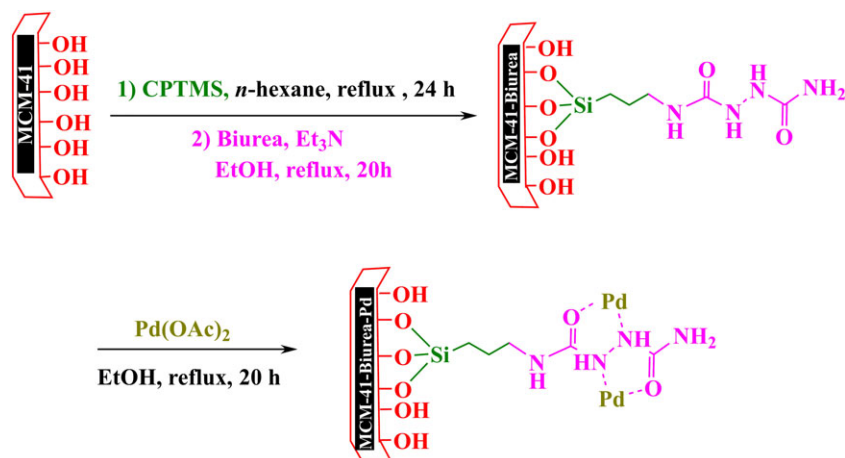


FIGURE 1 XRD patterns of MCM-41, MCM-41-CPTMS, MCM-41-CPTMS-Biurea and MCM-41-CPTMS-Biurea-Pd.

Pd. The FT-IR spectrum of the MCM-41 (Figure 2a) indicated absorption bands at 790–1060 and 445 cm^{-1} corresponding to the Si–O and Si–O–Si stretching frequencies, respectively. Also the band at 3450 cm^{-1} is assigned to the stretching vibration of the O–H groups. The bands appearing at around 2900 cm^{-1} in the spectrum of MCM-41-CPTMS correspond to (C–H) stretching vibrations (Figure 2b). In the FT-IR spectrum of MCM-41-CPTMS-Biurea (Figure 2c), the bands observed at 1610 cm^{-1} (C–N) and 1695 cm^{-1} (C=O) emphasize that biurea was successfully linked in the channels of the mesoporous material. Finally, in Figure 2(d) is recognized the formation of the palladium complex.

The morphology of MCM-41 and MCM-41-CPTMS-Biurea-Pd were investigated using scanning electron microscopy (SEM; Figure 3). As evident from the SEM images, the morphology of MCM-41-CPTMS-Biurea-Pd (Figure 3b) is analogous to the particle form of MCM-41 (Figure 3a). From the TEM image (Figure 3c), highly ordered long-range hexagonal arrangement of the pores



SCHEME 1 Synthesis of MCM-41-CPTMS-Biurea-Pd.

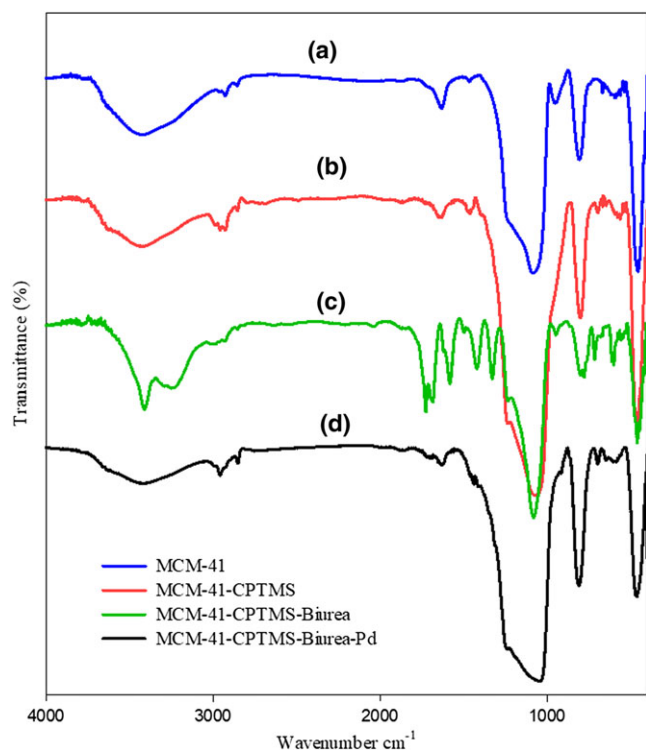


FIGURE 2 FT-IR spectra of (a) MCM-41, (b) MCM-41-CPTMS, (c) MCM-41-CPTMS-Biurea and (d) MCM-41-CPTMS-Biurea-Pd.

is clearly observed. It should be mentioned that the TEM observations and the XRD patterns are in good agreement with each other.

The energy-dispersive X-ray spectroscopy (EDS) results of the mesoporous complex are shown in Figure 4. As can be seen from these data Si, O, C, N and Pd elements have been detected in MCM-41-CPTMS-Biurea-Pd. Furthermore, the exact amount of Pd in MCM-41-CPTMS-Biurea-Pd was measured using inductively coupled plasma optical emission spectrometry (ICP-OES). From this analysis, the amount of Pd in MCM-41-CPTMS-Biurea-Pd is found to be 12.64%.

Thermogravimetric analysis (TGA) was also used to obtain information about weight changes of chemisorbed organic functional groups on the mesoporous material upon heating (Figure 5). The TGA plots of all samples display a slight weight loss below 200 °C, due to desorption of physically adsorbed solvents and surface hydroxyl groups of the catalyst. Also, the second weight loss, starting from 200 to 800 °C, is due to the thermal decomposition of functionalized organic moieties of the catalyst.

As evident in Figure 6, to determine the textural properties, the nitrogen adsorption–desorption isotherms of MCM-41 and MCM-41-CPTMS-Biurea-Pd samples were measured using the Brunauer–Emmett–Teller (BET) technique. The BET surface area, pore diameter and total pore volumes were determined for these samples and the results of this study are summarized in Table 1. When Pd

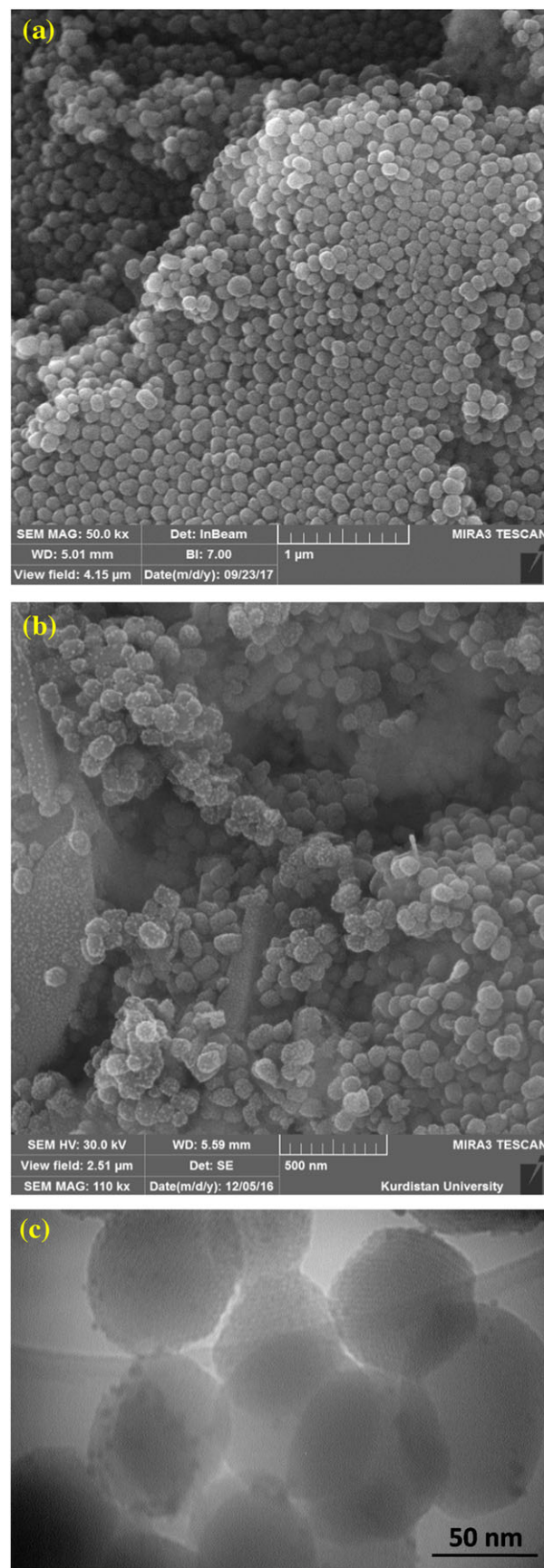


FIGURE 3 SEM images of (a) calcined MCM-41 and (b) MCM-41-CPTMS-Biurea-Pd. (c) TEM image of MCM-41-CPTMS-Biurea-Pd.

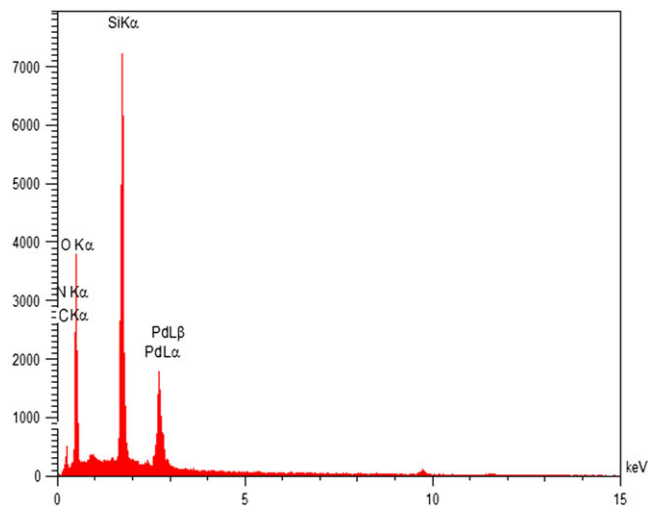


FIGURE 4 EDS spectrum of MCM-41-CPTMS-Biurea-Pd.

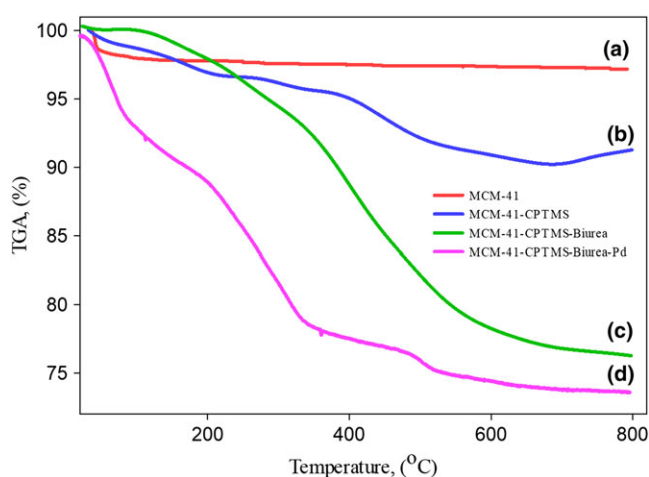


FIGURE 5 TGA thermograms of (a) MCM-41, (b) MCM-41-CPTMS, (c) MCM-41-CPTMS-Biurea and (d) MCM-41-CPTMS-Biurea-Pd.

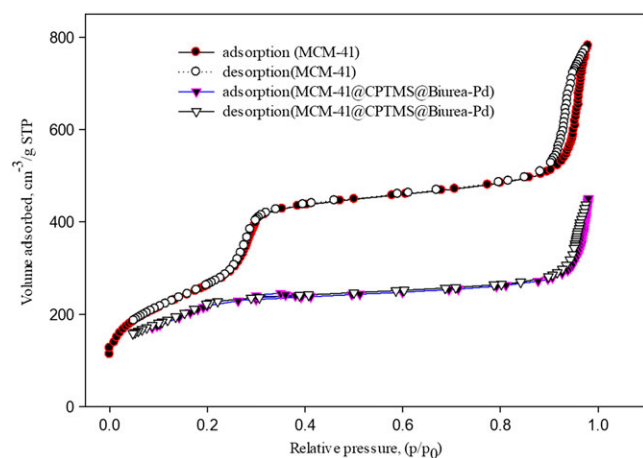


FIGURE 6 BET curves for (a) MCM-41 and (b) MCM-41-CPTMS-Biurea-Pd.

is loaded on MCM-41, specific pore volume and surface area decrease and wall diameter increases compared to MCM-41. These data are related to the presence of the Pd complex on the inner surface of MCM-41.

2.2 | Application of MCM-41-CPTMS-Biurea-Pd Complex in C–C Coupling Reaction

Our organic program involved examination of the catalytic activity of MCM-41-CPTMS-Biurea-Pd as an efficient and recyclable nanocatalyst in various Stille coupling reactions (C–C, C–N and C–O) and development of a simple and eco-friendly method. At the onset of the work we examined the reaction between aryls with Ph_3SnCl using various solvents, bases, temperatures and amounts of catalyst (Table 2). To find the optimum conditions, a model reaction was selected of iodobenzene and Ph_3SnCl in the presence of various amounts of MCM-41-CPTMS-Biurea-Pd.

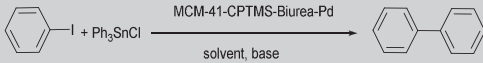
In the first step, to determine the optimum amount of catalyst, various amounts were utilized. As evident from Table 2 (entry 1), the coupling reaction does not proceed in the absence of catalyst after 18 h, and optimum amount of the catalyst was 5 mg (Table 2, entry 2). Among various bases, such as Et_3N , *N*-methylmorpholine and K_2CO_3 (Table 2, entries 2, 8 and 9), K_2CO_3 is more effective for this coupling reaction (Table 2, entry 2). This reaction was investigated using various solvents including dimethylformamide (DMF), EtOAc, CH_2Cl_2 , poly(ethylene glycol) (PEG) and *N*-methylpyrrolidone (NMP), and excellent yield was obtained in PEG (Table 2, entry 2). Optimization of temperature for this reaction shows that room temperature is the best choice. The effect of the amount of Ph_3SnCl was also evaluated (Table 2, entries 2, 10 and 11). The best result was achieved with 0.5 mmol of Ph_3SnCl (Table 2, entry 2). The results of these investigations are summarized in Table 2. Applying 1.0 mmol of aryl halide, 0.5 mmol of Ph_3SnCl and 2 mmol of K_2CO_3 in the presence of 5 mg of MCM-41-Biurea-Pd in 2 ml of PEG as solvent at room temperature (Table 2, entry 2) represents the best conditions for C–C coupling reactions.

Under the obtained optimized conditions, coupling of various types of aryl halides by Ph_3SnCl was examined. The results are summarized in Table 3. Aryl halides with various functional groups (electron-withdrawing and electron-donating groups) are well coupled with Ph_3SnCl to afford products in high yields (Table 3, entries 4 and 7). Another important aspect of this method is the successful reaction of aryl halides with steric effect. For instance α -bromonaphthalene could give product in good yields (Table 3, entries 5 and 8).

TABLE 1 Textural properties of MCM-41 and MCM-41-CPTMS-Biurea-Pd

Sample	S_{BET} ($\text{m}^2 \text{g}^{-1}$)	Pore diameter by BJH method (nm)	Pore volume ($\text{cm}^3 \text{g}^{-1}$)	Wall diameter (nm)
MCM-41	990	3.2	1.3	1.1
MCM-41-CPTMS-Biurea-Pd	400	1.6	0.6	3.0

TABLE 2 Optimization of parameters for C–C coupling reaction catalysed by MCM-41-CPTMS-Biurea-Pd^a

							
Entry	Cat. (mg)	Solvent	Ph ₃ SnCl	Base	Temp. (°C)	Time (h)	Yield (%) ^b
1	—	PEG	0.5	K ₂ CO ₃	r.t.	18	0
2	5	PEG	0.5	K ₂ CO ₃	r.t.	2.2	96
3	7	PEG	0.5	K ₂ CO ₃	r.t.	5	92
4	5	EtOAc	0.5	K ₂ CO ₃	r.t.	9	55
5	5	CH ₂ Cl ₂	0.5	K ₂ CO ₃	r.t.	8	57
6	5	NMP	0.5	K ₂ CO ₃	r.t.	9	48
7	5	DMF	0.5	K ₂ CO ₃	r.t.	6	47
8	5	PEG	0.5	Et ₃ N	r.t.	9	53
9	5	PEG	0.5	<i>N</i> -methylmorpholine	r.t.	3	41
10	5	PEG	0.3	K ₂ CO ₃	r.t.	7	61
11	5	PEG	1	K ₂ CO ₃	r.t.	5	90
12	5	PEG	0.5	K ₂ CO ₃	50	3.5	94
13	5	PEG	0.5	K ₂ CO ₃	90	3.5	92

^aReaction conditions: 1 mmol of iodobenzene and 2 mmol of K₂CO₃ in 2 ml of solvent.

^bIsolated yield.

After successful synthesis of various biphenyl compounds, we studied the catalytic activity of MCM-41-CPTMS-Biurea-Pd for C–N coupling reaction. For optimization of the reaction conditions, reaction of aniline (1 mmol) with Ph₃SnCl (0.5 mmol) was used as a model reaction in the presence of catalyst. The experiments show that applying 5 mg of nanocatalyst and Et₃N as base in PEG as solvent at 90 °C represents the best conditions for C–N bond formation (Table 4, entry 2).

The reaction of Ph₃SnCl was carried out with a variety of amines and the results obtained are summarized in Table 5. This methodology is applicable for amines with both electron-donating groups (Table 5, entries 2–5) and electron-withdrawing groups (Table 5, entry 6) in the reaction with Ph₃SnCl.

In final part of this project, to obtain the optimal reaction conditions for C–O coupling reactions, the reaction of phenol with Ph₃SnCl using various bases, solvents, temperatures and amounts of catalyst was studied (Table 6). Hence, the best result is achieved by conducting the reaction with phenol (1 mmol), Ph₃SnCl

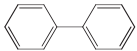
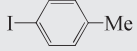
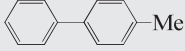
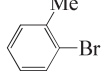
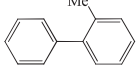
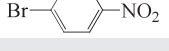
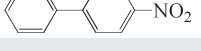
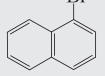
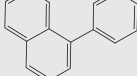
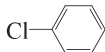
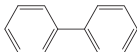
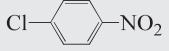
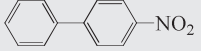
(0.5 mmol), Et₃N (2 mmol) and 5 mg of catalyst in PEG at 90 °C (Table 6, entry 2).

The reactions of various phenol derivatives, including those with electron-donating and electron-withdrawing groups, with Ph₃SnCl were studied. In all cases the reaction gives the products in good to excellent yields. The obtained results are summarized in Table 7.

2.3 | Recyclability of Nanocatalyst

Finally, the recyclability and reusability of the nanocatalyst were studied in C–C, C–N and C–O coupling reactions. In this manner, after reaction completion for each run, the catalyst was separated from the reaction mixture by simple centrifugation and washed with ethanol and water several times and then placed into a fresh reaction mixture. As shown in Figure 7, the MCM-41-CPTMS-Biurea-Pd was reused over six times without any significant palladium leaching or loss of its catalytic activity. Based on ICP-OES measurements, the amount

TABLE 3 Coupling of aryl halides with Ph_3SnCl catalysed by MCM-41-CPTMS-Biurea-Pd at room temperature

Entry	Aryl halide	Product ^a	Time (h)	Yield (%) ^b	M.p. (°C)
1			2.2	96	66–68 ^[34]
2			4.5	94	42–44 ^[35]
3			3	93	66–68 ^[34]
4			4	90	42–44 ^[35]
5			5	89	Colourless oil ^[34]
6			6	92	87–89 ^[34]
7			2	95	112–114 ^[34]
8			8	88	Oil ^[34]
9			5	89	66–68 ^[34]
10			4	91	112–114 ^[34]

^aThe products were identified and characterized by comparison of their physical and spectral data with those of authentic samples.

^bIsolated yield.

TABLE 4 Optimization of parameters for C–N coupling reaction catalysed by MCM-41-CPTMS-Biurea-Pd^a

						
Entry	Cat. (mg)	Solvent	Base	Temp. (°C)	Time (h)	Yield (%) ^b
1	—	PEG	Et_3N	90	24	—
2	5	PEG	Et_3N	90	12	96
3	7	PEG	Et_3N	90	11.5	91
4	5	EtOAc	Et_3N	Reflux	24	50
5	5	CH_2Cl_2	Et_3N	Reflux	24	45
6	5	DMF	Et_3N	90	20	67
7	5	—	Et_3N	r.t.	22	81
8	5	PEG	K_2CO_3	90	24	-
9	5	PEG	Et_3N	r.t.	18	63
10	5	PEG	Et_3N	60	15	75

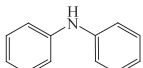
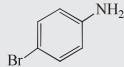
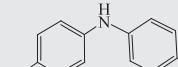
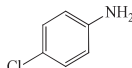
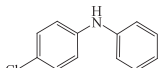
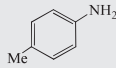
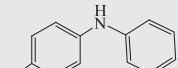
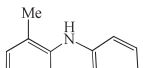
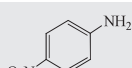
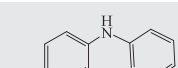
^aReaction conditions: 1 mmol of aniline with 0.5 mmol of Ph_3SnCl and 2 mmol of Et_3N in 2 ml of solvent.

^bIsolated yield.

of Pd was determined for unreacted catalyst (12.64%) and after the sixth run (12.5%). Based on EDS measurements, the amount of Pd was determined for unreacted catalyst (30.42 wt%) and after the sixth run (29.50 wt%) (Figure 8). Also, the nature of the recovered catalyst

was investigated using FT-IR spectroscopy (Figure 9), XRD (Figure 10), BET measurements (Figure 11) and SEM and TEM (Figure 12). FT-IR, SEM, TEM and XRD results for the recovered catalyst indicate that the catalyst can be recycled six times without any significant change

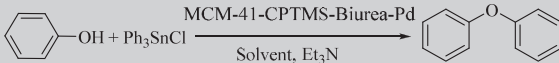
TABLE 5 Coupling of amines with Ph_3SnCl catalysed by MCM-41-CPTMS-Biurea-Pd at 90 °C

Entry	Amine	Product ^a	Time (h)	Yield (%) ^b	M.p. (°C)
1			12	96	55–56 ^[36]
2			11	92	88–90 ^[36]
3			16	84	73–75 ^[37]
4			17	81	89 ^[38]
5			20	75	38 ^[38]
6			9	94	135–136 ^[38]

^aThe products were identified and characterized by comparison of their physical and spectral data with those of authentic samples.

^bIsolated yield.

TABLE 6 Optimization of parameters for C–O coupling reaction catalysed by MCM-41-Biurea-Pd^a

					
Entry	Cat. (mg)	Solvent	Temp. (°C)	Time (h)	Yield (%) ^b
1	—	PEG	90	24	—
2	5	PEG	90	19	92
3	7	PEG	90	19	90
4	5	EtOAc	Reflux	40	37
5	5	CH_2Cl_2	Reflux	35	44
6	5	DMF	90	28	49
7	5	NMP	Reflux	38	53
8	5	—	90	30	52
9	5	PEG	r.t.	30	37
10	5	PEG	60	15	62

^aReaction conditions: 1 mmol of phenol with 0.5 mmol of Ph_3SnCl and 2 mmol of Et_3N in 2 ml of solvent.

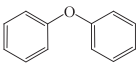
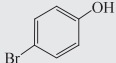
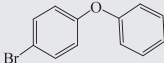
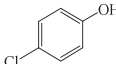
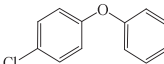
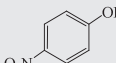
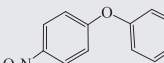
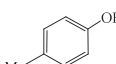
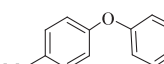
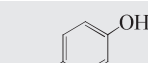
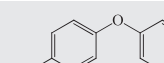
^bIsolated yield.

in its structure or mesoporosity of silicate parent. Morphological changes after the sixth run were investigated using SEM (Figure 12a). Figure 12(b) show a TEM image of representative regions of recovered MCM-41-CPTMS-Biurea-Pd and highly ordered long-range hexagonal arrangement of the pores can be clearly observed after six recycles of MCM-41-CPTMS-Biurea-Pd. In order to determine the textural properties of recovered MCM-41-CPTMS-Biurea-Pd after six recycles, the nitrogen adsorption and desorption isotherms were obtained as shown in

Figure 11. The BET surface area and the pore diameter were also determined for the catalyst recovered after the sixth run (Table 8), results indicating agreement with the textural properties of fresh MCM-41-CPTMS-Biurea-Pd (Table 1) and the surface area and pore size were retained at the end of the sixth recycling process. BET analysis of recovered MCM-41-CPTMS-Biurea-Pd shows a surface area of $450 \text{ m}^2 \text{ g}^{-1}$ and a pore volume of $0.61 \text{ cm}^3 \text{ g}^{-1}$.

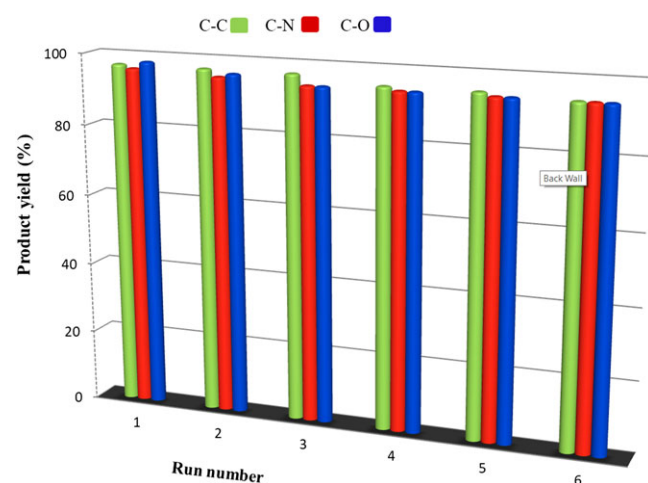
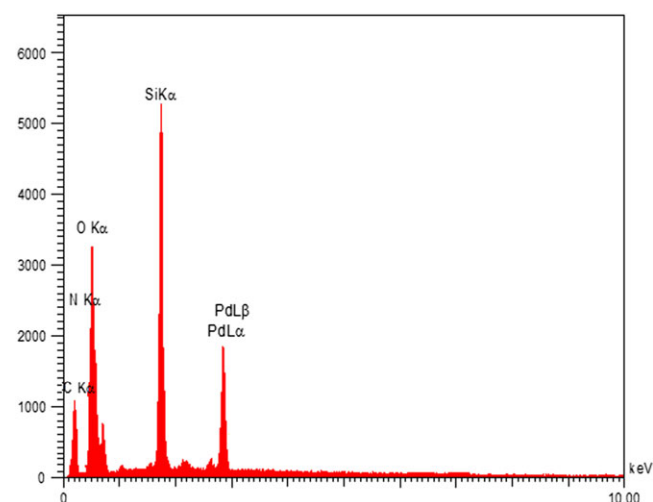
To examine the leaching of palladium in the reaction mixture and the heterogeneity of the catalyst, we

TABLE 7 Coupling of phenol derivatives with Ph_3SnCl catalysed by MCM-41-CPTMS-Biurea-Pd at 90 °C

Entry	Phenol	Product ^a	Time (h)	Yield (%) ^b	M.p. (°C)
1			19	92	Yellowish oil ^[39]
2			18	90	Yellowish oil ^[40]
3			21	86	Yellowish oil ^[40]
4			15	96	55–57 ^[41]
5			22	89	Yellowish oil ^[42]
6			24	90	Yellowish oil ^[42]

^aThe products were identified and characterized by comparison of their physical and spectral data with those of authentic samples.

^bIsolated yield.

**FIGURE 7** Reusability of MCM-41-Biurea-Pd.**FIGURE 8** EDS pattern of recovered MCM-41-CPTMS-Biurea-Pd.

performed hot filtration for the synthesis of diphenylamine with aniline and triphenyltin chloride. In this experiment, we obtained the yield of product in half the time of the reaction of 55%. Then, the reaction was repeated and in half the time of the reaction, the catalyst was separated and the filtrate allowed to react further. We found that, after this hot filtration, no further reaction was observed. The yield of reaction in this stage was 55%, confirming the leaching of palladium was negligible.

Comparison of the results with those for other catalysts shows a better catalytic activity of MCM-41-CPTMS-Biurea-Pd in C–C, C–N and C–O coupling reactions (Table 9). Many catalysts have been reported for C–C, C–N and C–O coupling reactions, such as benzothiazole-based Pd(II) complexes, *trans*-dichlorobis(triphenylphosphine)palladium(II), *N,N*-dimethylformamide-stabilized palladium nanoclusters, $\text{Cu}(\text{OAc})_2$, Cu -*N,N'*-bis(salicylidene)arylmethanediamine complex, CuI , *N,N*-dimethylglycine and CuO . Some of these methodologies have drawbacks or limitations such as the use of homogeneous catalysts that are difficult to separate from the reaction mixture, hazardous organic solvents, high temperature and long reaction times. Here, we used a silica-supported material that has advantages of low cost, ease of preparation and catalyst recyclability without significant loss of catalytic activity, and showing excellent catalytic activity for the C–C, C–N and C–O coupling reactions. Here, our catalytic system has important features such as using commercially available, eco-friendly, cheap and chemically stable materials and ease of preparation of the nanocatalyst by a simple procedure from silica-supported reagents and palladium as a

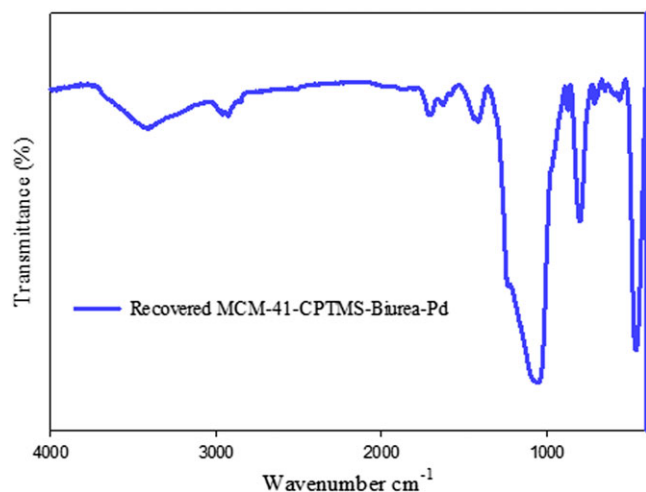


FIGURE 9 FT-IR spectrum of recovered MCM-41-CPTMS-Biurea-Pd.

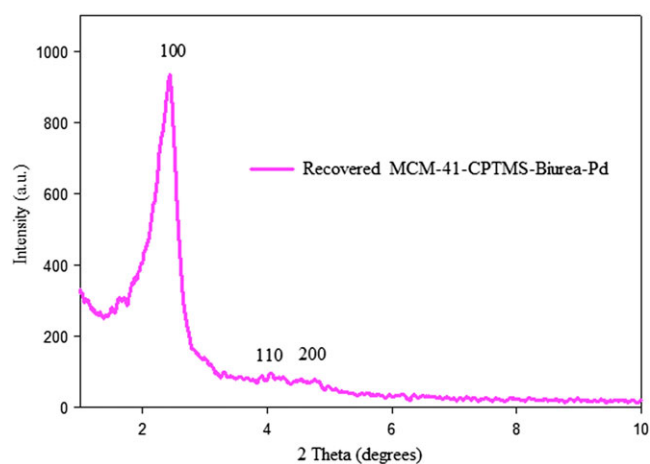


FIGURE 10 Low-angle XRD pattern of recovered MCM-41-CPTMS-Biurea-Pd.

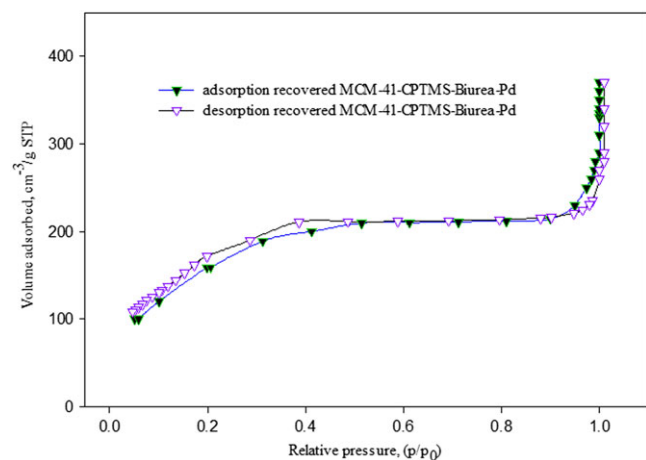


FIGURE 11 Nitrogen adsorption-desorption isotherms of recovered MCM-41-CPTMS-Biurea-Pd.

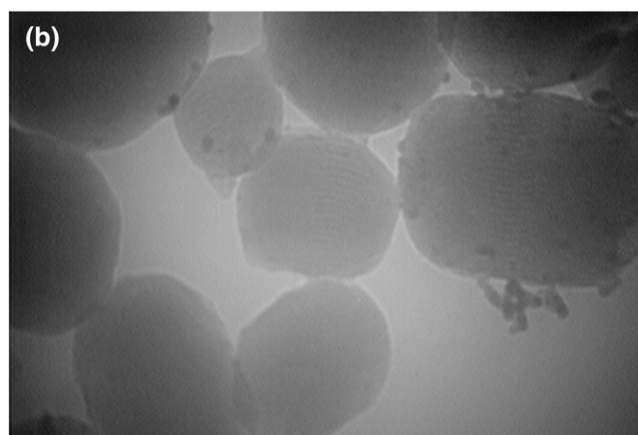
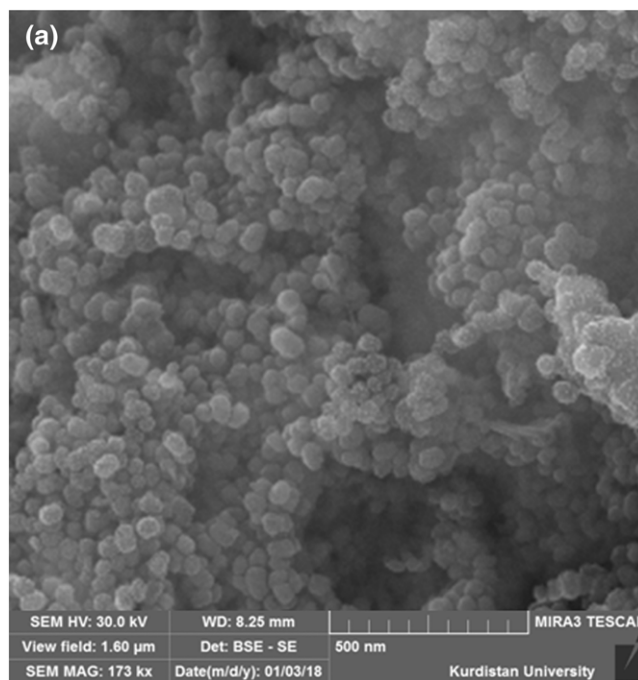


FIGURE 12 (a) SEM image and (b) TEM image of recovered MCM-41-CPTMS-Biurea-Pd.

transition metal and catalyst recycling without considerable decrease in activity. As evident from Table 9, MCM-41-CPTMS-Biurea-Pd is the best catalyst for C–C, C–N and C–O coupling reactions.

3 | EXPERIMENTAL

3.1 | Materials and Instrumentation

All the chemicals and solvents used in this work were obtained from Merck, Aldrich and Fluka and utilized without any purification. Using a Nexus 670 FT-IR spectrometer (Urmia University, Urmia, Iran), FT-IR spectra were obtained with KBr pellets. For reaction monitoring over silica gel SIL G/UV₂₅₄ plates, TLC was applied. The

TABLE 8 Textural parameters deduced from nitrogen sorption isotherms

Sample	S_{BET} ($\text{m}^2 \text{g}^{-1}$)	Pore diameter by BJH method (nm)	Pore volume ($\text{cm}^3 \text{g}^{-1}$)	Wall diameter (nm)
Recovered MCM-41-CPTMS-Biurea-Pd	450	1.60	061	2.95

TABLE 9 Comparison of activity of various catalysts reported in the literature in C–C, C–N and C–O coupling reactions

Entry	Catalyst	Temp. (°C)	Solvent	Time (h)	Yield (%)	Ref.
1	MCM-41-CPTMS-Biurea-Pd	r.t.	PEG	2.2	96 ^a	This work
2	Benzothiazole-based Pd(II) complexes	100	H ₂ O	1	100 ^a	[43]
3	<i>trans</i> -Dichlorobis(triphenylphosphine) palladium(II)	90	PEG	0.5	68 ^a	[44]
4	<i>N,N</i> -Dimethylformamide-stabilized palladium nanoclusters	120	NMP/DMF	15	72 ^a	[45]
5	MCM-41-CPTMS-Biurea-Pd	90	PEG	12	96 ^b	This work
6	Cu(OAc) ₂	r.t.	Et ₃ N	24	94 ^b	[41]
7	Cu– <i>N,N</i> -bis(salicylidene)arylmethanediamine complex	r.t.	H ₂ O	15	91 ^b	[46]
8	MCM-41-CPTMS-Biurea-Pd	90	PEG	19	96 ^c	This work
9	Cu(OAc) ₂	r.t.	Et ₃ N	30	85 ^c	[41]
10	CuI, <i>N,N</i> -dimethylglycine	90	Dioxane	16	86 ^c	[47]
11	CuO	120	DMSO	20	86 ^{c,d}	[48]

^aC–C coupling reaction.^bC–N coupling reaction.^cC–O coupling reaction.^dUnder nitrogen.

particle morphology was investigated using SEM (University of Kurdistan, Sanandaj, Iran) with a Tescan MIRA3. With a Bruker NMR spectrometer, ¹H NMR spectra (400 and 250 MHz) were recorded. TGA curves were obtained using a Shimadzu DTG-60 instrument (University of Kurdistan, Sanandaj, Iran). In addition, EDS analysis done was using a Tescan MIRA3 (University of Kurdistan, Sanandaj, Iran). TEM analysis of the catalyst was conducted using a Zeiss EM10C TEM (K. N. Toosi University of Technology, Tehran, Iran). Powder XRD patterns were collected using a Co radiation source with wavelength $\lambda = 1.78897 \text{ \AA}$, 40 kV with a Scintag PAD V X-ray diffractometer (Shahid Beheshti University, Tehran, Iran). The samples were scanned in the range $2\theta = 1\text{--}10^\circ$. Moreover, to determine material properties such as the catalyst surface area, pore volume and average pore diameter, nitrogen adsorption–desorption isotherms were measured using a standard gas manifold at 77 K (Sharif University of Technology, Tehran, Iran). Furthermore, adsorption data were obtained using the BET method. The content of Pd was measured using ICP-OES (Tarbiat Modares University, Tehran, Iran). Finally, TEM analysis of the catalyst was done using a

Zeiss-EM10C TEM (K. N. Toosi University of Technology, Tehran, IRAN). It should be mentioned that PEG with a molecular weight of 400 was used in all reactions.

3.2 | Preparation of Siliceous MCM-41

According to the method presented elsewhere,^[49] mesoporous Si-MCM-41 was synthesized through a sol–gel procedure. The steps of the synthesis procedure of Si-MCM-41 were as follows. In a typical procedure, firstly, a solution containing 480 ml of deionized water and 3.5 ml of NaOH (2 M) was stirred at 80 °C. Next, 1.0 g (2.74 mmol) of surfactant cetyltrimethylammonium bromide was added if the solution became homogeneous. Afterwards, 5 ml of tetraethyl orthosilicate was slowly added dropwise into the solution which led to a white slurry. After that the obtained mixture was refluxed at the same temperature under continuous stirring for 2 h. Finally, to remove the remaining surfactant and obtain the mesoporous Si-MCM-41, the collected product was filtered, washed with deionized water and dried in an oven at 70 °C followed by calcination at 550 °C for 5 h with a ramp of 2 °C min^{−1}.

3.3 | Preparation of MCM-41-(CH₂)₃Cl

MCM-41 powder (4.8 g) with CPTMS (5.0 g) was added to *n*-hexane (96 ml). In this step, the mixture was stirred under reflux and nitrogen atmosphere for 24 h. The obtained solid was collected by filtration, washed with *n*-hexane several times and finally dried under vacuum. In this way, MCM-41-(CH₂)₃Cl was obtained.

3.4 | Preparation of MCM-41-CPTMS-Biurea

A mixture of MCM-41-CPTMS (1 g), biurea (1 g) and Et₃N (2 ml) in ethanol (50 ml) was stirred under reflux for 20 min in a 100 ml round-bottom flask. Afterwards, by washing the obtained product several times with dry ethanol and drying it in vacuum oven at 60 °C for 12 h, the preparation stage was finished.

3.5 | Preparation of MCM-41-CPTMS-Biurea-Pd

In the first step, the functionalized MCM-41 (MCM-41-Biurea) (3 g) was mixed with Pd(OAc)₂ (1 g) in ethanol (50 ml) and the obtained material was stirred under reflux for 20 h. In the second step, to remove any unanchored metal ions, the resulting blue solid was filtered off, washed several times with ethanol and dried in vacuum at 60 °C for 12 h. The obtained catalyst was designated MCM-41-CPTMS-Biurea-Pd.

3.6 | General Procedure for C–C Coupling Reaction of Aryl Halides with Triphenyltin Chloride

A mixture of aryl halide (1 mmol), triphenyltin chloride (0.5 mmol), K₂CO₃ (2 mmol) and MCM-41-CPTMS-Biurea-Pd (5 mg) was stirred in PEG at room temperature and the progress of the reaction was monitored by TLC. After reaction completion, the mixture was cooled to room temperature, and the nanocatalyst was separated by filtration and washed with ethanol and water. The mixture was diluted with EtOAc (4 × 5 ml) and water, the extracted organic layer was dried over MgSO₄ and the solvent was evaporated to afford pure biphenyl product.

3.7 | General Procedure for C–N Coupling Reaction of Anilines with Triphenyltin Chloride

To a stirred solution of aniline (1 mmol), triphenyltin chloride (0.5 mmol) and Et₃N (2 mmol) in PEG (2 ml)

was added MCM-41-CPTMS-Biurea-Pd (5 mg) at 90 °C. The progress of the reaction was monitored by TLC. The catalyst was separated by filtration and reused as such for the next experiment. The mixture was washed with EtOAc (4 × 5 ml) and water, and then the extracted organic layer was dried over MgSO₄ and solvent was evaporated to afford the product.

3.8 | General Procedure for C–O Coupling Reaction of Phenol with Triphenyltin Chloride

Phenol (1 mmol), triphenyltin chloride (0.5 mmol) and Et₃N (2 mmol) in PEG (2 ml) were added to MCM-41-CPTMS-Biurea-Pd (5 mg) and the mixture was stirred at 90 °C, the progress of the reaction being monitored using TLC. After completion of the reaction, the catalyst was separated by filtration. The mixture was washed with EtOAc (4 × 5 ml) and water, and then the extracted organic layer was dried over MgSO₄ and solvent was evaporated to afford the product.

4 | CONCLUSIONS

We successfully designed a new mesoporous metal complex (MCM-41-CPTMS-Biurea-Pd) and used it as a catalyst for C–C, C–N and C–O bond formation through the reaction of triphenyltin chloride as a phenyl source with various phenyl halides, arylamines and phenols in a green solvent. This nanocatalyst was characterized using several techniques such as XRD, FT-IR spectroscopy, BET measurements, TGA, SEM, TEM, EDS and ICP-OES. The main advantages of this catalytic system are easy preparation, high stability and reusability of the catalyst, green conditions, short reaction times, easy workup, simple purification and high yields of products.

ORCID

Nader Noroozi Pesyan  <http://orcid.org/0000-0002-4257-434X>

REFERENCES

- [1] V. Polshettiwar, R. S. Varma, *Green Chem.* **2010**, *12*, 743.
- [2] K. S. W. Sing, D. H. Everett, R. A. W. Haul, L. Mouscou, R. A. Pierotti, J. Rouquerol, T. Siemieniowska, *Pure Appl. Chem.* **1985**, *57*, 603.
- [3] M. Yoshikazu, Y. Masanori, A. Eiichi, A. Sadao, T. Shunsuke, *Ind. Eng. Chem. Res.* **2009**, *48*, 938.
- [4] F. Torney, B. G. Trewyn, V. S. Y. Lin, K. Wang, *Nat. Nanotechnol.* **2007**, *2*, 295.

- [5] M. Hajjami, F. Ghorbani, F. Bakhti, *Appl. Catal. A* **2014**, *470*, 303.
- [6] L. Lv, K. Wang, X. S. Zhao, *J. Colloid Interface Sci.* **2007**, *305*, 218.
- [7] R. M. Martin-Aranda, J. Cejka, *Top. Catal.* **2010**, *53*, 141.
- [8] I.I. Slowing, J.L. Vivero-Escoto, C.W. Wu, V.S.Y. Lin, *Adv. Drug Delivery Rev.* **2008**, *60*, 1278.
- [9] X. Hu, G. K. Chuah, S. Jaenicke, *Appl. Catal. A* **2001**, *217*, 1.
- [10] M. Hajjami, L. Shiri, A. Jahanbakhshi, *Appl. Organometal. Chem.* **2015**, *29*, 668.
- [11] G. Karthikeyan, A. Pandurangan, *J. Mol. Catal. A* **2009**, *311*, 36.
- [12] M. Mandal, V. Nagaraju, B. Sarma, G. V. Karunakar, K. K. Bania, *ChemPlusChem* **2015**, *80*, 749.
- [13] W. Xiaoli, Z. Fang, W. Gongde, L. Xianfeng, X. Yunbo, D. Keqiang, *Catal. Lett.* **2013**, *143*, 219.
- [14] S. Bhunia, D. Saha, S. Koner, *Langmuir* **2011**, *27*, 15322.
- [15] V. Mahdavi, M. Mardani, M. Malekhosseini, *Catal. Commun.* **2008**, *9*, 2201.
- [16] J. Sreyashi, D. Buddhadeb, B. Rajesh, K. Subratanath, *Langmuir* **2007**, *23*, 2492.
- [17] H. Batmani, N. Noroozi Pesyan, F. Havasi, *Micropor. Mesopor. Mater.* **2018**, *257*, 27.
- [18] F. Havasi, A. Ghorbani-Choghamarani, F. Nikpour, *New J. Chem.* **2015**, *39*, 6504.
- [19] C. Barnard, *Platinum Met. Rev.* **2008**, *52*, 38.
- [20] B. Khakiani, K. Pourshamsian, H. Veisi, *Appl. Organometal. Chem.* **2015**, *29*, 259.
- [21] H. Veisi, M. Pirhayati, A. Kakanejadifard, *Tetrahedron Lett.* **2017**, *58*, 4269.
- [22] H. Veisi, M. Ghadermazi, A. Naderi, *Appl. Organometal. Chem.* **2016**, *30*, 341.
- [23] M. Pirhayati, H. Veisi, A. Kakanejadifard, *RSC Adv.* **2016**, *6*, 27252.
- [24] H. Veisi, P. Mohammadi Biabri, H. Falahi, *Tetrahedron Lett.* **2017**, *58*, 3482.
- [25] F. Heidari, M. Hekmati, H. Veisi, *J. Colloid Interface Sci.* **2017**, *501*, 175.
- [26] X. F. Wu, P. Anbarasan, H. Neumann, M. Beller, *Angew. Chem. Int. Ed.* **2010**, *49*, 9047.
- [27] K. C. Nicolaou, P. G. Bulger, D. Sarlah, *Angew. Chem. Int. Ed.* **2005**, *44*, 4442.
- [28] C. Torborg, M. Beller, *Adv. Synth. Catal.* **2009**, *351*, 3027.
- [29] A. Ghorbani-Choghamarani, F. Nikpour, F. Ghorbani, F. Havasi, *RSC Adv.* **2015**, *5*, 33212.
- [30] D. Astruc, F. Lu, J. R. Aranzaes, *Angew. Chem. Int. Ed.* **2005**, *44*, 7852.
- [31] D. E. Bergbreiter, P. L. Osburn, J. D. Frels, *J. Am. Chem. Soc.* **2001**, *123*, 11105.
- [32] J. M. Zhou, R. X. Zhou, L. Y. Mo, S. F. Zhao, X. M. Zheng, *J. Mol. Catal.* **2002**, *178*, 289.
- [33] M. Opanasenko, P. Stepnicka, J. Cejka, *RSC Adv.* **2014**, *4*, 65137.
- [34] L. Bai, J. X. Wang, *Adv. Synth. Catal.* **2008**, *350*, 315.
- [35] Z. Du, W. Zhou, F. Wang, J. X. Wang, *Tetrahedron* **2011**, *67*, 4914.
- [36] L. Rout, P. Saha, S. Jammi, T. Punniyamurthy, *Adv. Synth. Catal.* **2008**, *350*, 395.
- [37] K. W. Anderson, M. Mendez-Perez, J. Priego, S. L. Buchwald, *J. Org. Chem.* **2003**, *68*, 9563.
- [38] X. Zhu, L. Su, L. Huang, G. Chen, J. Wang, H. Song, Y. Wan, *Eur. J. Org. Chem.* **2009**, *209*, 635.
- [39] H. J. Cristau, P. P. Cellier, S. Hamada, J. F. Spindler, M. Taillefer, *Org. Lett.* **2004**, *6*, 913.
- [40] V. Avudoddi, V. K. G. Palle, V. R. Pallapothula, *Eur. J. Chem.* **2012**, *3*, 298.
- [41] N. Iranpoor, H. Firouzabadi, E. Etemadi Davan, A. Rostami, A. Nematollahi, *J. Organometal. Chem.* **2013**, *740*, 123.
- [42] A. B. Naidu, E. A. Jaseer, G. Sekar, *J. Org. Chem.* **2009**, *74*, 3675.
- [43] K. M. Dawood, M. R. Shaaban, M. B. Elamin, A. M. Farag, *Arabian J. Chem.* **2017**, *10*, 473.
- [44] A. Ghorbani-Choghamarani, H. Babaei, M. Hashemi, B. Notash, *A. Naghipour., J. Organometal. Chem.* **2017**, *841*, 31.
- [45] H. Yano, Y. Nakajima, Y. Obora, H. Yano, *J. Organometal. Chem.* **2013**, *745*, 258.
- [46] A. Gogoi, G. Sarmah, A. Dewan, U. Bora, *Tetrahedron Lett.* **2014**, *55*, 31.
- [47] D. Ma, Q. Cai, *Org. Lett.* **2003**, *5*, 3799.
- [48] M. A. Khalilzadeh, H. Keipour, A. Hosseini, D. Zareyee, *New J. Chem.* **2014**, *38*, 42.
- [49] Q. Cai, Z. S. Luo, W. Q. Pang, Y. W. Fan, X. H. Chen, F. Z. Cui, *Chem. Mater.* **2001**, *13*, 258.

SUPPORTING INFORMATION

Additional supporting information may be found online in the Supporting Information section at the end of the article.

How to cite this article: Batmani H, Noroozi Pesyan N, Havasi F. Synthesis and characterization of MCM-41-Biurea-Pd as a heterogeneous nanocatalyst and using its catalytic efficacy in C–C, C–N and C–O coupling reactions. *Appl Organometal Chem.* 2018;e4419. <https://doi.org/10.1002/aoc.4419>